THE AMERICAN SOCIETY OF MECHANICAL ENGINEERS
345 E. 47 St., New York, N.Y. 10017

82-GT-117

A Computational Design Method for Transonic Turbomachinery Cascades

H. Sobieczky
Research Scientist,
DFVLR - Institut für
Theoretische Strömungsmechanik,
Göttingen, F.R. Germany

D. S. Dulikravich
Research Scientist,
NASA Lewis Research Center,
Cleveland, OH

This paper describes a systematical computational procedure to find configuration changes necessary to modify the resulting flow past turbomachinery cascades, channels and nozzles, to be shock-free at prescribed transonic operating conditions. The method is based on a finite area transonic analysis technique and the fictitious gas approach. This design scheme has two major areas of application. First, it can be used for design of supercritical cascades, with applications mainly in compressor blade design. Second, it provides subsonic inlet shapes including sonic surfaces with suitable initial data for the design of supersonic (accelerated) exits, like nozzles and turbine cascade shapes. This fast, accurate and economical method with a proven potential for applications to three-dimensional flows is illustrated by some design examples.

NOMENCLATURE

a	Speed of sound
A	Speed of sound, nondimensionalized with critical conditions
B	Determinant of the Jacobian: $\partial(x,y)/\partial(X,Y)$
c	Cascade chord length (Fig. 1);
C	Fictitious gas parameter
D	Density, nondimensionalized with critical conditions
g	Gap distance between cascade airfoils (Fig. 1)
K	Characteristics coefficient
M	Mach number
q	Velocity magnitude
Q	Velocity magnitude, nondimensionalized with critical conditions. (Laval number)
$r_{1,2}$	Leading and trailing edge radii (Fig. 1)
t	Thickness at mid-chord (Fig. 1)
u,v	Velocity components in physical plane (x,y)
U,V	Contravariant velocity components in computational plane (X,Y)
x,y	Coordinates of the flow (physical) plane
X,Y	Coordinates of the computational plane
$\alpha_{1,2}$	Flow angle, up- and downstream conditions
β	Cascade stagger angle (Fig. 1)
β_1	Leading edge angle (Fig. 1)
β_2	Trailing edge angle (Fig. 1)
γ	Ratio of specific heats
ν	Prandtl-Meyer turning angle
ϕ	Velocity potential
Ψ	Stream function
ρ	Fluid density
ϑ	Flow angle
ξ,η	Characteristics

Subscripts, superscripts

f	fictitious
is	isentropic
$*$	at critical conditions.

INTRODUCTION

Transonic flow in turbomachinery has become a field of increasing importance since requirements for higher engine thrust - to - weight ratio have forced the operating conditions of compressors and turbines into the regime of mixed subsonic - supersonic flow conditions. Since transonic flows are usually accompanied by shock waves which may adversely effect compressor/turbine efficiency due to wave drag, viscous interaction and unsteady effects, it is important for the design aerodynamicist to

Contributed by the Gas Turbine Division of the ASME.

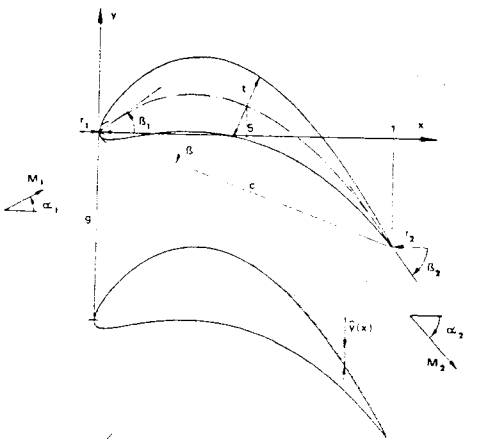

Fig. 1 Cascade geometry.

have computational tools for transonic airfoil-, cascade-, and channelflow analysis at hand which provide a reliable flow field analysis and a systematic approach to minimize the shock effects. This is analogous to the situation in aircraft design where tools for wing definition to obtain shapes with minimal drag for given lift are needed.

Following the experimental verification of nearly shock-free airfoil flows by Whitcomb[1] and Pearcey[2], computational tools were developed on the basis of analytical studies in the hodograph plane, to provide airfoil shapes with shock-free flow at specified design conditions. Garabedian and Korn[3] developed a numerical hodograph method for shock-free supercritical cascades. Though this method is mathematicallly elegant, it is too complicated for practical use in the turbomachinery industry.

In this paper, a method for cascade blade design is presented, which can be used also in an analysis mode to compute transonic flow fields through cascades with shocks. The design principles have been applied already to single airfoil design including viscous effects and three-dimensional wing design[4,5,6]. Such extensions are desirable and possible for turbomachinery applications, too.

A short description of cascade geometry, the numerical analysis algorithms and the incorporated "fictitious gas" - concept is given. Results for shock-free supercritical compressor cascades are illustrated by choice of a conventional cascade and the first steps of a design process leading to a useful redesign. Transition from shock-free to choked conditions is studied and a turbine cascade example is presented.

BLADE GEOMETRY GENERATOR

The method presented here provides local and relatively small shape modifications resulting from flow calculations past given "initial configurations". An analytical shape generator including a set of parameters to be flexible in creating blade shapes with some prescribed geometrical properties seems useful, (see Fig. 1). Analytical functions for camber and thickness distribution are defined by leading and trailing edge angles and radii, and by a thickness parameter.

These simple shapes may be modified locally by an additional set of parameters to create bumps or ramps on the surface, as illustrated by the shaded area in Fig. 1. These latter parameters allow small shape variations necessary to arrive at more suitable pressure distributions, as well as a modeling of viscous displacement effects if the design procedure is included in a coupled viscous - inviscid analysis algorithm. For the case of accelerated flows, the initial configuration may even have to have an open trailing edge (see Fig. 1) in order to arrive at a useful turbine cascade with a closed trailing edge. Finally, one may think of more global optimization procedures, with the shock-free design method included, where the shape-generating parameters are subject to systematic changes. All of this suggests analytical shape generation prior to flow field analysis.

COMPUTATIONAL GRID GENERATION

Numerical analysis used in this method is carried out in a computational domain which is a mapping of the physical 2D space into a rectangular region. Orthogonal grid lines of the computational plane map into nearly - orthogonal lines in the physical plane. The cascade airfoil shape and a suitably chosen periodicity line form boundaries in the computational plane. Figure 2 illustrates an "O"-grid around a compressor airfoil. Present results and experience have been obtained using this type of grid, but a "C"-grid is better suited to include viscous effects near the trailing edge by allowing introduction of an arbitrarily shaped constant thickness wake, see Figure 3.
The work here is on two-dimensional flow but the method has the potential to be extended into three dimensions to be a design tool for rotors, propellers etc. C-grids on coaxial cylinders are very useful in these cases where the wake has high influence on the flow.

FINITE AREA NUMERICAL ANALYSIS

A computational algorithm for the analysis of transonic flow through cascades was developed by Dulikravich[7,8].
A brief description of the method follows, in the case of steady, two-dimensional, irrotational isentropic flow of an inviscid, compressible fluid, the conservative form of the continuity equation is

$$(\rho u)_x + (\rho v)_y = 0. \qquad (1)$$

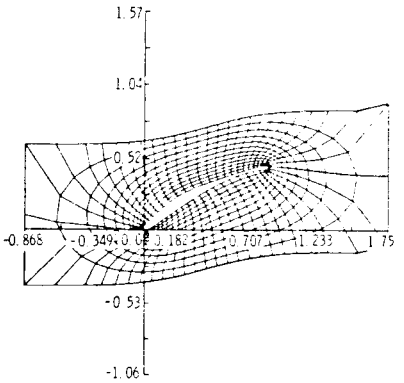

Fig. 2 Computational 'O'-type grid.

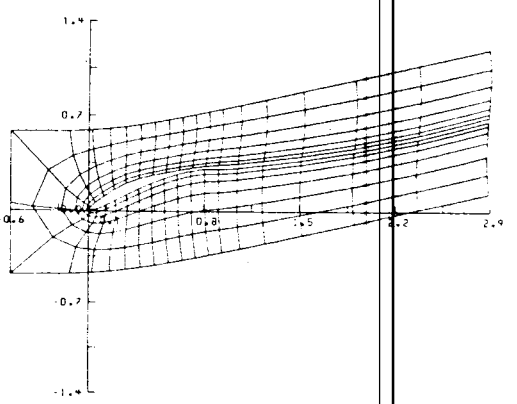

Fig. 3 Computational 'C'-type grid.

Equation (1) can also be expressed in its canonical operator form[9] as

$$\rho((1-M^2)\phi_{ss} + \phi_{nn}) = 0 , \qquad (2)$$

where (s,n) is the streamline aligned coordinate system. Equation (2) represents a quasi-linear, second-order partial differential equation of mixed elliptic-hyperbolic type that accepts isentropic discontinuities in its solution. These isentropic shocks satisfy mass conservation but differ from Rankine-Hugoniot shocks. Equation (1) is solved by using an iterative line over-relaxation scheme where consecutive iteration sweeps through the flow field are considered as steps in an artifical time direction.
Solution of this steady-state equation (1) is obtained as an asymptotic solution to an artificially unsteady equation

$$\rho((1-M^2)\phi^H_{ss} + \phi^E_{nn} + \xi\phi_{st} + \eta\phi_{nt} + \varepsilon\phi_t) = 0 \qquad (3)$$

for large times, where ξ,η and ε are constants.
Superscript H in equation (3) designates upstream differencing, and superscript E designates central differencing to be used for the evaluation of particular second derivatives. The steady part of equation (3) is always evaluated by using equation (1) supplemented by a directional numerical viscosity in a continuously fully conservative form, thus uniquely capturing isentropic shocks. Equation (2) is used only to construct a correction to the potential matrix.
For the purpose of a type-dependent[10], rotated[9] finite difference evaluation of the derivatives in equation (2) and a finite area[11] evaluation of the first derivatives in equation (1), the flow field and the governing equations are transformed from the physical (x,y) plane (Figures 2 or 3) into a rectangular (X,Y) computational domain by using local isoparametric bilinear mapping functions.

If the geometric transformation matrix is

$$[J]^T = \begin{bmatrix} x_X & y_X \\ x_Y & y_Y \end{bmatrix} , \qquad (4)$$

then the contravariant velocity components in the (X,Y) plane are

$$\begin{Bmatrix} U \\ V \end{Bmatrix} = [J]^{-1} \begin{Bmatrix} u \\ v \end{Bmatrix} = [J]^{-1}[J^T]^{-1} \begin{Bmatrix} \phi_x \\ \phi_y \end{Bmatrix} . \qquad (5)$$

Consequently the fully conservative form of the continuity equation (eq. (1)) becomes

$$\left((\rho UB + \delta')_X + (\rho VB + \delta'')_Y\right)/B = 0, \qquad (6)$$

where the artificial viscosity terms δ',δ'' represent principal parts of a truncation error of equation (2). The iterative solution process of equation(2) is accelerated by using a fourlevel, consecutive-grid refinement procedure.

All the flow parameters are nondimensionalized with respect to the critical conditions denoted by an asterisk so that the isentropic relations used for the local fluid density and the speed of sound are

$$D_{is} = \rho/\rho^* = \left((\gamma+1)/2-(\gamma-1)Q^2/2\right)^{1/(\gamma-1)}, \qquad (7)$$

$$A^2_{is} = a^2/a^{*2} = D_{is}^{\gamma-1}, \qquad (8)$$

with the nondimensional speed Q, a function of the local Machnumber

$$Q = q/a^* = M(\gamma+1)^{1/2}/(2+(\gamma-1)M^2)^{1/2}. \qquad (9)$$

SUPERCRITICAL FLOWS

Compressible flow past an airfoil in the high subsonic speed regime results in a more or

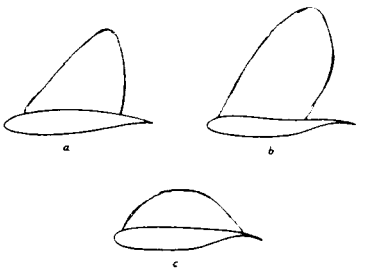

Fig. 4 Supercritical airfoil flows. Local supersonic regions with
a) shock on the surface,
b) shock in the flow
c) shock-free flow.

less pronounced local supersonic region usually terminated by a recompression shock. The shock wave forms in the flow field and ends vertically at the curved airfoil surface (Figure 4a). Viscous effects, however, complicate the flowfield in the footpoint region of the shock, a ramp-like thickening of the boundary layer leads to a shock-formation within the viscous layer, associated with a smearing of the steep pressure rise on the surface. A similar flow structure can occur in purely inviscid flow with a shock-formation in the flow-field, too.

This is of significance because design procedures prescribing a shock-free pressure distribution on the airfoil surface cannot necessarily guarantee entirely shock-free flow[12]. Resulting airfoil shapes have a concave suction surface and a shock-wave "hangs" in the flow field, (Figure 4b). Though performance of such an airfoil does not suffer from the negative effects of shock-boundary layer interaction at design conditions, wave drag is present and most likely off design conditions will lead to severe interaction problems.

Flows of practical interest exhibit not too extensive local supersonic regions being entirely shock-free, (Figure 4c). In the following idea use is made of the fact that this type of flow is qualitatively similar to entirely subsonic flow: no discontinuities of the flow properties disturb the smooth character of the flow. Subsonic (mathematically elliptic type) relations are, therefore, used to model a flow with a sonic line as sketched in Fig. 4c.

FICTITIOUS GAS FLOWS

A possibility to generate flows with shock-free local supersonic regions is - as a consequence of the qualitative relationship to subsonic flow - the method of elliptic continuation.
It was first used in hodograph (indirect) design procedures but its physical interpretation led to more practical nearly direct design methods. A theoretical background and examples of the method applied to transonic

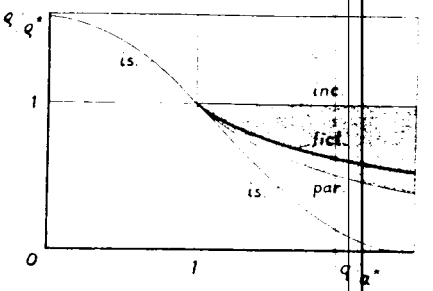

Fig. 5 Isentropic and fictitious gas density relations.

airfoil design is given by Sobieczky[13]. The idea is to make use of an existing flow analysis algorithm, which should, at least, be reliable for subsonic flows. The only necessary changes in such an algorithm are made in the formulas for density and speed of sound given above for isentropic flow, Eqs. (7) and (8). Relation (7) for density vs. velocity is drawn in Figure 5 (line 'is') Only the supercritical part $q \geq a^*$ is considered for alternative density-velocity relations which alter the supersonic (hyperbolic type) nature of the "real" isentropic flow into elliptic type "fictitious" supercritical gas flow. It can easily be shown that a density-velocity relation

$$D_f = \rho_f/\rho^* = Fct(Q) \tag{10}$$

with

$$d(D_f \cdot Q)/dQ > 0 \tag{11}$$

leads to an elliptic partial differential equation analogous to equation (1) but describing flows with properties (10).

The isentropic nature of the flow for subcritical velocities $Q < 1$ is maintained by forcing

$$D = \begin{cases} D_f(Q), & Q \geq 1, \\ D_{is}(Q), & Q \leq 1, \end{cases} \tag{12}$$

with smooth transition of D and its first derivative at sonic conditions:

$$Q^* = 1: \quad D^*_{is} = D^*_f = 1, \tag{13}$$

$$(dD_{is}/dQ)^* = (dD_f/dQ)^* = -1.$$

The speed of sound of this fictitious gas is determined by the general continuity criterion

$$A_f^2(Q) = - D_f \cdot Q/(dD_f/dQ). \qquad (14)$$

It is observed that $A_f > 1$ as long as the gradient of D_f is greater than the negative product of D_f and Q. For vanishing gradient the speed of sound goes to infinity and we have a locally incompressible nature of the flow. This singularity may cause difficulties in the analysis algorithm, so we observe the constraints

$$- D_f / Q < dD_f/dQ < 0. \qquad (15)$$

This relation restricts the fictitious domain of the diagram (Fig. 5) to the shaded area within D_{inc} = const. = 1 where the flow is incompressible with critical conditions, and $D_{par} = 1/Q$ where the gas is of parabolic type, with the local speed of sound equal to local velocity.

Different formulas for D_f have been tested so far. They seem mainly equivalent if their second derivative at sonic conditions is the same, i.e., if the coefficient C of the quadratic term in the near-sonic expansion

$$D_f(Q > 1) = 1 - (Q-1) + C\ (Q-1)^2 + \ldots \qquad (16)$$

is the same. In the cascade analysis code, formulas containing C as a free parameter are presently examined, for example the relations

$$D_f = (1+(2C-1)(Q-1))^{-1/(2C-1)},$$
$$A_f^2 = Q(1+(2C-1)(Q-1)), \qquad (17)$$

with $1 < C < \infty$ covering the whole shaded range in Fig. 5. With a choice of C within these limits the fictitious gas is defined quantitatively and with an analysis code a flow of this gas through a cascade can be calculated. The code is also extended to yield the shape of the sonic line(s) in the field, dividing the subcritical real isentropic part of the flow from the supercritical fictitious one. Also, the flow angles at the sonic line are determined.

We realize that an isentropic flow problem is solved locally where the speed is subcritical, but there are no real-flow results for the region of local supersonic flow. The fictitious part of the flow served to give a suitable sonic line consistent with shock-free flow.

CALCULATION OF THE SUPERSONIC FLOWFIELD

As previously described, the flow through a cascade is calculated using the correct equations when the flow is subsonic. The flow is isentropic up to the resulting sonic line, the solution is fixed and known there and so are the initial values to solve the hyperbolic equations.

For two-dimensional flow the method of characteristics is used in a hodograph - like working plane in which the characteristics are orthogonal straight lines. The hodograph variables are the flow angle ϑ and the Prandtl-Meyer turning angle

$$\nu(M) = h \cdot \arctan\left((M^2-1)^{1/2}/h\right) - \arctan (M^2-1)^{1/2} \qquad (18)$$

with

$$h^2 = (\gamma+1)/(\gamma-1). \qquad (19)$$

In the working plane ν and ϑ may be chosen using arbitrary functions of the characteristics ξ,η

$$\nu = F(\xi) + G(\eta),$$
$$\vartheta = F(\xi) - G(\eta). \qquad (20)$$

The velocity potential and stream function then satisfy

$$\Phi_\xi = K(\nu(\xi,\eta))\ \Psi_\xi,$$
$$\Phi_\eta = -K(\nu(\xi,\eta))\ \Psi_\eta, \qquad (21)$$

or, equivalently

$$(d\Psi/d\Phi)_{\xi,\eta = \text{const.}} = \pm K^{-1}, \qquad (22)$$

where the $\pm$ signs refer to ξ,η = const, respectively. The coefficient K is a function of the Mach number also, therefore with $\nu(M)$ a function of ξ,η,

$$K(\nu) = K(\nu(M)) = (1+(\gamma-1)M^2/2)^{1/(\gamma-1)} \cdot (M^2-1)^{1/2}. \qquad (23)$$

Values for the velocity potential Φ on the parabolic line, and the shape of this line are used along with the usual relations between the physical coordinates x,y and Φ,Ψ to find Ψ on the sonic line. These initial data are then integrated using (22) to determine the locus $\Psi(x,y) = 0$ which passes through the intersection of the sonic line with the airfoil shape. The values of y for

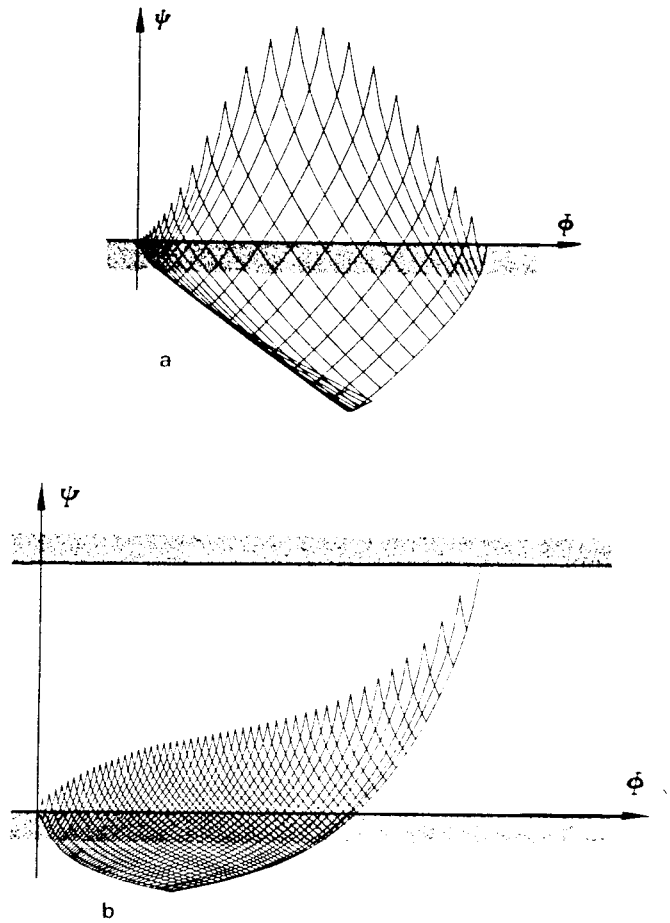

Fig. 6 Supersonic characteristics in the plane of potential φ and stream-function ψ.
a) Supercritical shock-free flow,
b) accelerated flow.

which $\psi(x,y) = 0$ determine the new airfoil shape. This shape will have the same slope and, at least theoretically, the same curvature, as the initial surface at the sonic points.

Two different types of initial data may occur in cascade flows: supercritical and choked flows. A solution for a local supersonic domain on a supercritical cascade is illustrated in the φ,ψ-plane (Figure 6a). The grid lines drawn are the characteristics, sonic line data are given on the arc formed by their cusps, the solution extends into the airfoil surface represented by the shaded φ-axis. An overlapped region is observed within this extended domain. If this reaches into the flowfield above $\psi=\psi$(surface), the solution along with the previously obtained subsonic part of the flow cannot be used for design of a physically meaningful shock-free flow. Initial configuration and/or design operating conditions have to be changed in order to suppress occurrence of such "limit lines" in the physical flow field.

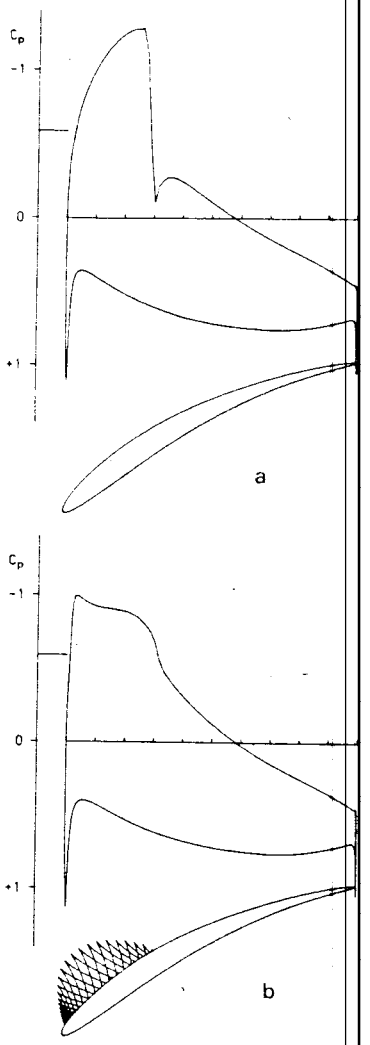

Fig. 7 Design modifications of a given compressor cascade at $M_1 = 0.75$, $M_2 = 0.476$, $\Delta\alpha = 24°$, $g/c = 1.1$,
a) Analysis of flow past given cascade
b) Redesign for shock-free flow.

In the case of choked flow the sonic line extends from one cascade blade to the next. In the φ,ψ-plane (Fig. 6b) the sonic line is now a curve between the stream-function levels of two neighbouring cascade airfoils. Only a part of the lower surface wetted by supersonic flow is determined as in the supercritical case and the supersonic domain is now open toward downstream direction. Solution data on the exit characteristic form the necessary input to start a supersonic characteristics calculation downstream.

The choking sonic line may have a normal tangent in the φ,ψ-plane, the flow has then the character of an accelerated Laval-nozzle and the characteristic grid consists of two more or less symmetrical parts of the kind shown in Fig. 6b.

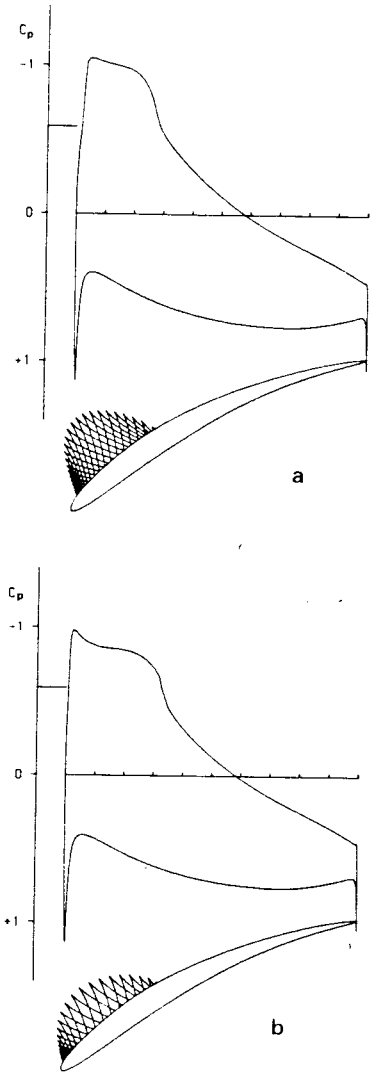

Fig. 8 Influence of fictitious gas parameter C. Fictitious gas
a) near parabolic limit,
b) near elliptic limit.

COMPRESSOR CASCADE DESIGN EXAMPLE

The first steps of shock-free design of a compressor cascade are described briefly to aid the turbomachinery designer in understanding the flexibility of this technology. Conditions for a realistic transonic operation, (here:

$M_1 = 0.75$, $\alpha_1 = 41°$, $\alpha_2 = 17°$)

and a blade geometry by fixing parameters for the airfoil generation is chosen. Next the analysis (original) version of the finite area algorithm is used to determine quality of the flow near the leading and trailing edges.

Slight variations of the leading and trailing edge angles to obtain smooth flow conditions finally gives angles

$\beta = 27.3°$, $\beta_1 = 45°$, $\beta_2 = 10.7°$.

Gap to chord ratio and thickness of the blade at midchord were chosen to $g/c = 1.1$, $t/c = 0.055$.

Figure 7a shows the blade geometry and analysis pressure coefficient obtained for the given operating conditions. The flow has a very strong shock, viscous flow would never allow for such a solution. Then the design version of the computer code with fictitious gas and a parameter C = 25 is used. The result includes a plot of the characteristics in the redesigned supersonic domain. It shows a smooth, shock-free flow through the cascade, the airfoils are flattened in the region from 3 to 40 percent chord on the suction surface. Maximum thickness reduction is less than 0.5 percent chord, in the present plot this can barely be seen. As mentioned above a value for the fictitious gas parameter C was chosen, but a large range of C was examined to study its influence on the quality of the obtained shock-free flows.

Figure 8 illustrates extreme results: Fig. 8a shows a nearly parabolic fictitious gas (C = 3). A short but high supersonic field is observed while for a nearly incompressible fictitious gas (C = 400, Fig. 8b) a longer but flatter supersonic region is obtained. The latter case has a more pronounced peaky pressure distribution which is favorable for off design performance but disadvantageous for the viscous flow: transition will occur at the pressure peak, too early on airfoil chord so that the shock-free but still steep recompression area near midchord will lead to turbulent separation. It is seen here that the flexibility to vary the solution by simply changing the gas parameter is rather limited. We return, therefore, to the first choice of C = 25 and fix this value while looking for other, more powerful tools to influence the flow quality. Very effective are geometrical changes of the initial airfoil prior to the shock-free design modification in order to soften the upper surface pressure peak and steep gradient. A bump - provided by the additional set of parameters in the blade generator - on the upper surface between leading edge and 80% chord brings some favorable changes (Figure 9a):

1. The resulting blade is 1.5% chord thicker which is desirable for structure.
2. The pressure suction peak near the leading edge is reduced, boundary layer calculations at a Reynolds number of one million indicate a downstream shift of transition from laminar to turbulent flow, from 8 to 40% chord.
3. The steep pressure rise at mid-chord is softened so that boundary layer separation does not occur before 99% chord, close to the trailing edge.

Further improvements of this cascade are obtained mainly in the trailing edge region.

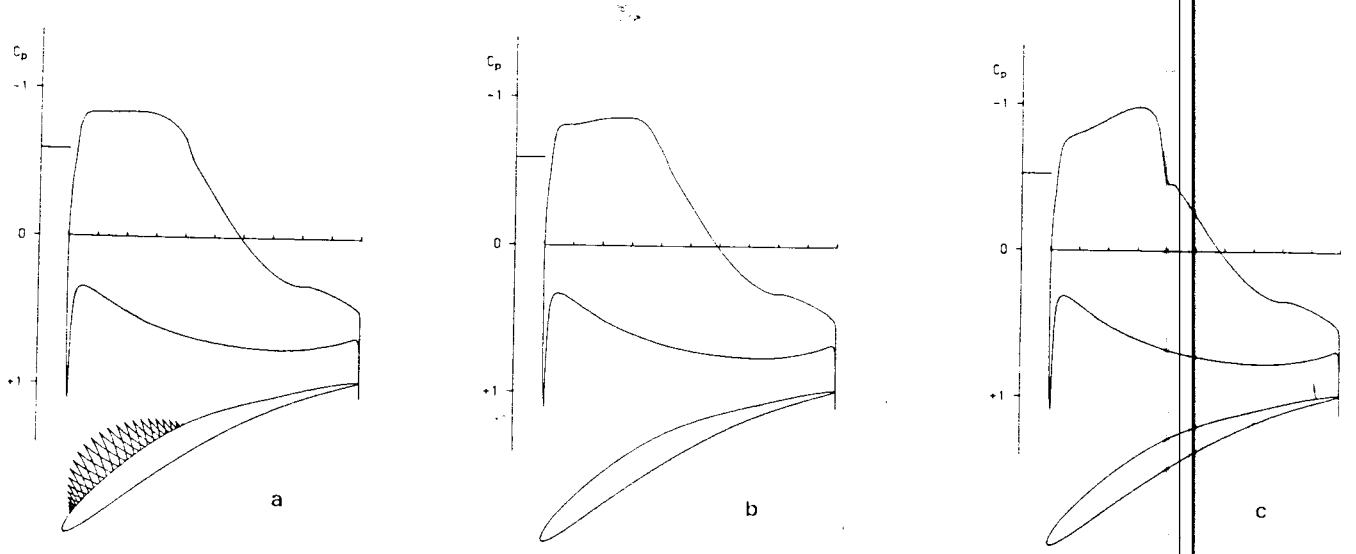

Fig. 9 Improved design
a) by addition of a bump prior to design.
b) Analysis verification of shock-free flow at design conditions ($M_1 = 0.75$).
c) Off design analysis at $M_1 = 0.77$.

A lift and increased curvature of the whole tail area give still better Stratford-type pressure distribution[14]. Here it is intended to show that subsonic design technology can be applied to transonic flows, without major complications usually occurring in computations of this speed regime.

Finally inviscid analysis results are shown for the last design, Fig. 9. The code is switched from design to analysis and the designed cascade coordinates are used as input for analysis at the same operating conditions. Figure 9b shows excellent agreement with the shock-free design pressure distribution. Off design performance of this cascade should be investigated including interaction, too. An airfoil analysis code was extended by a shock-boundary layer interaction computation[15], the algorithm can easily be introduced into this code. Fig. 9c shows inviscid off-design analysis at $M_1 = 0.77$, the shock-wave is still much weaker than the one occurring on the original cascade (Fig. 7a) at $M_1 = 0.75$.

TRANSITION TO CHOKING CONDITIONS

Increasing the upstream Mach number of a cascade flow will eventually lead to choked conditions, where the flow has no longer local supersonic regions but accelerates to supersonic speeds with sonic lines extending from one to the next airfoil. This flow occurs in turbine cascades, it is a further subject of our work to provide design codes for such flows. Before the procedure is illustrated, an interesting question should be answered:

How do local supersonic shock-free regions merge when choking conditions are approached?

To answer this question an unstaggered cascade of NACA 0012 airfoils with a gap-to-chord ratio of one is defined. Analysis results by various authors say this cascade will choke at a Mach number $M_1 \approx 0.65$. At a Mach number of $M_{1crit} < 0.644$ the flow is still subcritical. The design version of our cascade code is used now for shock-free redesign of this cascade. Results for different Mach numbers $M_1 > M_{1crit}$ were obtained, until choking finally occurred at $M_{1L} = 0.669$. This illustrates how the design thickness reduction (about 0.5 percent of NACA 0012, with a fictitious gas parameter $C = 25$) pushes the choking Mach number up nearly $\Delta M = 0.02$.

Figure 10 shows the design result at $M_1 = 0.668$, immediately before choking. Sonic lines for different Mach numbers between critical conditions (where sonic conditions are reached at point C) and nearly choking are plotted. The limiting case, where the supersonic regions just merge, cannot be traced with the numerical algorithm, but an analytical investigation by Sobieczky[16] shows that the sonic line ends in a cusp formed by two parabola lines. The subsonic flow disintegrates in two parts, with the analytical behavior following accelerated and decelerated Laval-nozzle solutions in the upstream and downstream part of the flow, respectively. The Laval-nozzle flow extends beyond the sonic line down- und upstream to the limiting characteristics, which are parabolas too. Only a narrow region at the vertical axis through

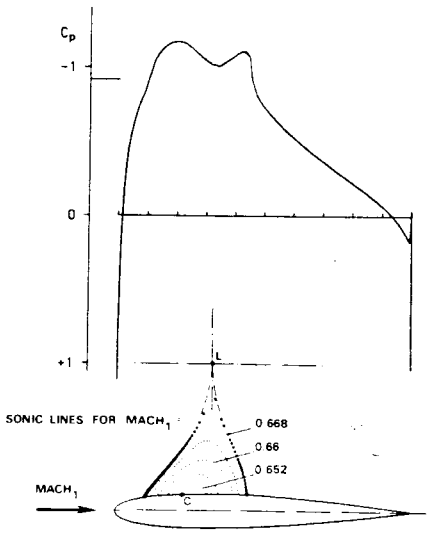

Fig. 10 Supercritical shock-free flow approaching choked conditions.

point L contains a different solution connecting the two Laval-nozzle-type flows. The resulting flow has a jump from positive to equal negative acceleration at the horizontal axis through L, but at other levels velocity or pressure has a characteristic dip which is observed already at near-choking conditions on the airfoil.

This flow analysis has mainly academic value, but it illustrates the transition to accelerated flow. One can abandon the whole symmetrical and decelerated parts of the flow without disturbing the upstream accelerated flow. The flow can be continued by a supersonic exit construction method, starting at the limiting characteristic. In the case of the NACA cascade this means, that the nose of the NACA 0012 airfoil stays unchanged from 0 to about 10 percent chord. A smooth thickness reduction starts then until the limiting expansion characteristic starts at about 24 percent and runs into Laval point L. Downstream of 24 percent the airfoil may be changed allowing supersonic expansion, e.g. for a supersonic parallel flow exit design.

ACCELERATED CASCADE FLOWS

A Laval-nozzle type of flow usually occurs only in cascades or channels with low turning angle with boundaries forming a throat with walls of opposite sign curvatures. Turbine cascade flows with high curvature have no throat point L, transition from supercritical flow to choked conditions takes place without the above discribed singularity.

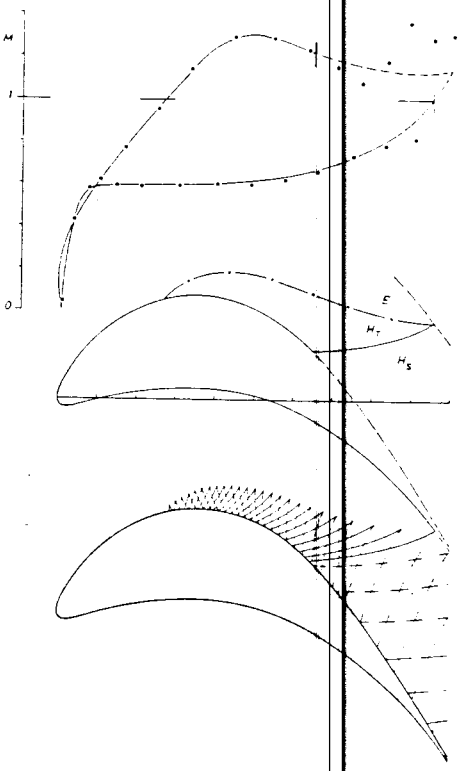

Fig. 11 Turbine cascade test example. Redesign based on experimental results (Heinemann, DFVLR), $M_1 = 0.39$, $M_2 = 1.15$, $\Delta\alpha = 79°$, $g/c = 0.5$.

A test example of this kind, Figure 11, was computed with an earlier hodograph method to provide a suitable sonic line for supersonic exit calculations. It is a turbine cascade just above choking conditions, the example is derived from existing test results obtained by Heinemann[17] at the DFVLR. Subsonic flow (domain E in Fig. 11) was verified by the hodograph method[13] equivalent to a fictitious gas analysis result. The method of characteristics determines now at first the transonic region (H_T) of supersonic flow, the solution of this example is illustrated in the ϕ,Ψ-plane in Figure 6b. The supersonic exit (H_S) was designed following the experimentally tested cascade shape. The obtained solution agrees very well to the measured values of surface Mach number exept in the supersonic exit, where weak shocks were found in experiment.

CONCLUSION

A new and simple method for determining turbomachinery cascades which are shock-free at prescribed operation conditions is described. The systematic computational procedure provides geometrical changes necessary to make a conventional compressor cascade perform efficiently at transonic flow speeds.

The present version computer codes include a design- and analysis algorithm for supercritical compressor cascades and a program for transonic inlet design for choked channel or cascade flows. The codes are based on the finite volume and fictitious gas concepts and the method of characteristics. A flexible cascade geometry generator and automatic multi-level boundary - conforming computational grid generation are included. In combination with viscous flow analysis an efficient optimization algorithm can be developed, furthermore the method has a potential for applications to three-dimensional flows in turbomachinery and past propellers.

REFERENCES

1 Whitcomb, R.T. and L. Clark, "An Airfoil Shape for Efficient Flight at Supercritical Mach numbers", NASA TM X-1109 (1965).

2 Pearcey, H.H., "The Aerodynamic Design of Section Shapes for Swept Wings", Advances in Aeronautical Sciences, Vol 3 (1962).

3 Garabedian, P.R. and Korn, G., "Numerical Design of Transonic Airfoils", Numerical Solution to Partial Differential Equations, Vol. II-SYNSPADE 1970, Academic Press, New York, (1978), pp. 253-271.

4 Sobieczky, H., N.J. Yu, K.-Y. Fung, A.R. Seebass, "New Method for Designing Shock-free Transonic Configurations", AIAA Journal Vol. 17 No. 7 (1979).

5 Nebeck, H.E., A.R. Seebass, H. Sobieczky, "Inviscid-viscous interactions in the nearly-direct design of shock-free supercritical airfoils", AGARD FDP Symposium on computation of viscous/inviscid interaction, CP 291 (1980).

6 Fung, K.-Y., H. Sobieczky, A.R. Seebass "Shock-free Wing Design", AIAA Journal Vol. 18, Nr. 10, pp. 1153-1158 (1980).

7 Dulikravich, D.S., "CAS2D-Fortran Program for Nonrotating Blade-to-Blade, Steady, Potential Transonic Cascade Flows", NASA TP-1705, (1980).

8 Dulikravich, D.S., "Numerical Calculation of Inviscid Transonic Flow Through Rotors and Fans", Ph.D. Thesis, Cornell Univ., (1979). Avail. Univ. Microfils, Order No. 7910741, 300 N. Zeeb Rd., Ann Arbor, MI, 48106.

9 Jameson, A., "Transonic Flow Calculations", in Computational Fluid Dynamics Vol. 1, Von Karman Institute VKI-LS-87-VOL-1, (1976), pp. 1.1-5.84.

10 Murman, E.M. and Cole, J., "Calculation of Plane Steady Transonic Flows", AIAA Journal, Vol. 9, (1971), pp. 114-121.

11 Jameson, A. and Caughey, D., "A Finite Volume Scheme for Transonic Potential Flow Calculations", AIAA 3rd Computational Fluid Dynamics Conference, (1977), Paper 77-635, pp. 35-54.

12 Volpe, G., R.E. Melnik, "The Role of Constraints in the Inverse Design Problem for Transonic Airfoils", AIAA paper 81-1233, (1981).

13 Sobieczky, H., "Related Analytical, Analog and Numerical Methods in Transonic Airfoil Design", AIAA-paper 79-1556, (1979).

14 Sobieczky, H., Dulikravich, D.S., "Design Exmaples for Supercritical Cascades", to be published as DFVLR report, (1982).

15 Nandanan, M., E. Stanewsky, G.R. Inger, "A Computational Procedure for Transonic Airfoil Flow Including a Special Solution for Shock Boundary Layer Interaction", AIAA-paper 80-1389, (1980).

16 Sobieczky, H., "Transonic Design Aerodynamics", Lecture Series, NASA-Lewis Research Center, June 1981.

17 Heinemann, H.-J., "Experimentelle Untersuchungen an hoch belasteten Schaufelgitter-Profilen", DFVLR-AVA report 251-73 C 09 (1973).